Jet Impingement Cooling in Power Electronics for Electrified Automotive Transportation: Current Status and Future Trends

Samantha Jones-Jackson, *Student Member, IEEE*, Romina Rodriguez, *Member, IEEE*, and Ali Emadi, *Fellow, IEEE*

***Abstract*—Effective thermal management of power electronics in electric vehicles is essential for reliability and increased power density. Currently, traditional cooling technologies such as cold plates and heat sinks have been utilized by the automotive industry. As the next generation of power electronics implements wide-bandgap devices, however, increased heat fluxes will require more advanced cooling strategies. Recently, jet impingement has gained attention as an advanced cooling technique for power electronics due to its proven thermal performance in high-heat-flux applications. This article aims to review the state-of-the-art jet impingement designs applied for power electronics cooling, as well as review future jet impingement technology. Important factors for widespread implementation such as heat transfer, pressure drop, and reliability are discussed, along with the current technical gaps and challenges for jet impingement research in electrified transportation.**

***Index Terms*—Cooling, electric vehicles, electrified powertrains, heat flux, inverters, jet impingement, power electronics.**

I. Introduction

IN ORDER to make electric vehicles competitive in the market, there is a substantial amount of research to increase the efficiency and power density of power electronics [1]. While silicon insulated-gate bipolar transistors (IGBTs) are common in electric vehicle power modules, there is an increasing trend toward implementing wide-bandgap (WBG) devices, such as silicon carbide (SiC) and gallium nitride (GaN), because of reduced losses [2], [3]. The usage of these WBG devices allows for increased current and voltage ratings of the semiconductor power devices.

However, increasing the power output in the electric components while decreasing the packaging size will result in additional thermal management challenges that need to be mitigated. The resulting increased heat flux can cause several issues, such as decreased reliability, decreased efficiency, and potentially even failure. The decreased reliability and efficiency are directly correlated with the higher conduction losses at higher temperatures, since the total resistance between the source and the drain, i.e., $R_{\mathrm{DS(on)}}$, is a function of temperature [4], [5]. Often, the module failure occurs because of either thermal cycling, which causes fatigue at the interfaces between the power modules' layers, or when exceeding the maximum allowable temperature, which causes burnout of the dies [6], [7]. Since temperature is the predominant cause of failure in power electronics [8], [9], as shown in Fig. 1, implementing an adequate cooling solution is crucial to reliability.

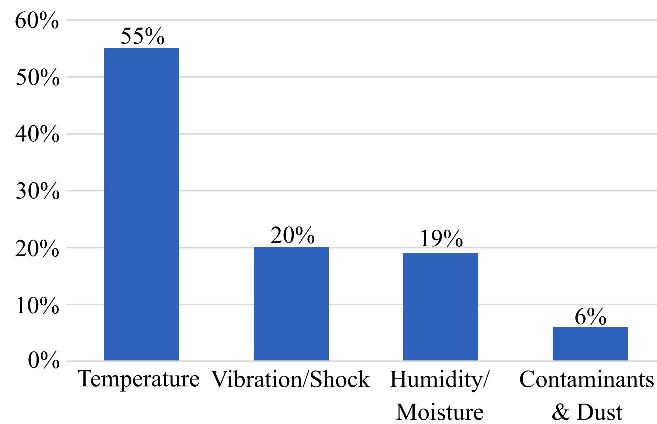

Fig. 1. Causes of failure in power electronic systems [9].

Although the term power electronics refers to converters/inverters and the components in them, the highest dissipators of heat are the semiconductor switches, which exist as both discrete switches and power modules. Both these components generate consolidated hotspots and require localized cooling strategies. With semiconductor chips as the main heat source, the cooling efforts should be focused on these concentrated heat loads.

To help reduce temperature-related failures within power electronic modules, currently, there are several thermal management solutions, including cold plates, heat sinks, air cooling, and liquid jets [8]. Typically, IGBT modules are cooled with horizontal flow cooling channels or cold plates [10]. This horizontal path can occur linearly or in a serpentine style, moving back and forth [11]. However, as there is a trend toward WBG devices that operate at high switching frequencies and are expected to dissipate at least 1000 W/cm^2 [12], with current devices reaching 500 W/cm^2 [13], high-heat-flux technologies

Manuscript received August 13, 2020; revised January 4, 2021; accepted February 10, 2021. Date of publication February 16, 2021; date of current version June 1, 2021. Recommended for publication by Associate Editor J. Wang. *(Corresponding author: Samantha Jones-Jackson.)*

The authors are with the McMaster Automotive Resource Centre, McMaster University, Hamilton, ON L8P 0A6, Canada (e-mail: jonesjas@mcmaster.ca; romina@mcmaster.ca; emadi@mcmaster.ca).

Color versions of one or more figures in this article are available at https://doi.org/10.1109/TPEL.2021.3059558.

Digital Object Identifier 10.1109/TPEL.2021.3059558

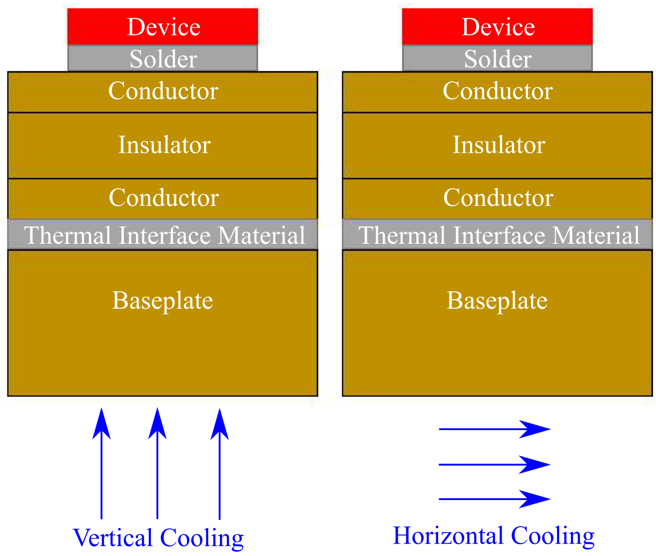

Fig. 2. Power electronic module material layers, with a direct bonded copper.

will be necessary. Horizontal flow cooling strategies generally produce heat transfer coefficients up to 20 000 W/m^2·K, but vertical cooling strategies, such as jet impingement, can reach up to 115 000 W/m^2·K [14]. A common layout for power electronic modules with horizontal and vertical cooling is shown in Fig. 2.

Although vertical cooling methods, such as jet impingement, have proven increased thermal performance [15], it is not widely implemented for power electronics cooling, mainly due to its relatively higher pressure drop [16]. However, these pressure losses can be reduced, and research has been conducted for a wide range of thermal management applications such as solar applications [17]–[21], turbines [22]–[25], food industry [26], motors [27], and electronic chips [28], [29]. Research is well documented on jet impingement for cooling applications, with specific focus on the effects of jet parameters on cooling effectiveness. Most studies have examined the effects of the jet diameter [14], [28]–[35], the nozzle to plate spacing [28]–[31], [33], [34], spacing between jets [31], the number of jets [14], and different jet orifice geometries [17], [36], [37]. Other studies investigate multiple jets versus single jets [31] and free-surface jets compared to submerged jets [28], [29], [38], [39], as well as sprays [40]–[43], and synthetic jets [44]–[46]. The cooling performance is typically reported with the nondimensional Nusselt number, Nu, and the heat transfer coefficient for various Reynolds numbers and volumetric flow rates, in order to compare these different design parameters.

This article aims to review the different types of jet impingement cooling that have a potential to be implemented in power electronics cooling for electrified transportation applications. Although the physics and thermal management properties of jet impingement have been extensively studied, this article presents current literature on power electronic applications, which has not been reviewed before. State-of-the-art cooling methods for automotive power electronics have been reviewed extensively, with focus on high-temperature power modules [10] and traditional cooling techniques [47]; however, none have reviewed jet impingement. Generally, jet impingement is discussed as a future trend of power electronics cooling, but since implementation of WBG technology will result in higher heat dissipation, a review of jet impingement cooling technology for power electronics is essential. As power modules are the main heat dissipating devices, they will be the focus of this article. The organization of this article is as follows. Section II describes the physical properties of different types of jets and their importance to power module applications. The heat transfer, pressure drop, reliability, and integration of jet impingement with power modules are reviewed in Section III. The advanced jet impingement technology is outlined in Section IV, and the technical gaps and challenges for future jet impingement in electrified transportation are detailed in Section V. Finally, Section VI concludes the article.

II. Jet Characteristics

Various types of jets have been proposed and can generally be divided into free surface, submerged, confined, and synthetic (pulsating) jets. The following sections will review the literature on jet impingement and briefly describe the flow mechanisms and physical properties for each type of jet. The heat transfer and flow for jet impingement can generally be nondimensionalized to compare performance of different jet designs.

A. Nondimensional Groups

In general, the thermal performance of a proposed cooling technology is characterized and reported through various nondimensional numbers. Nondimensional numbers are easily applied to simplified models or as boundary conditions to evaluate the potential performance of a technology.

The most common nondimensional number for reporting the convective heat transfer performance is the Nusselt number Nu, which considers the fluid properties, as well as the heat transfer coefficient. The Reynolds number, Re, is used to indicate whether the jet fluid flow is laminar, transitional, or turbulent. Depending on the application of these nondimensional numbers, different characteristic lengths can be used (e.g., jet diameter and radial distance from the jet) and are chosen by the author reporting the performance. The Nusselt number and Reynolds number are, respectively, defined as

$$Nu = \frac{hL_c}{k} \tag{1}$$

$$Re = \frac{\rho V L_c}{\mu} \tag{2}$$

where h is the heat transfer coefficient, described in (5), L_c is the characteristic length, k is the thermal conductivity of the fluid, ρ is the fluid density, V is the jet velocity, and μ is the dynamic viscosity.

Another important nondimensional number is the Strouhal number, St. Although it is less common, it is used when analyzing unsteady or oscillating jet impingement and is defined as follows:

$$St = \frac{fL_c}{u_j} \tag{3}$$

where f is the pulsation frequency and u_j is the time-averaged jet velocity. The Strouhal number is used to compare different nozzle designs and different types of pulsations between jets.

Finally, another important nondimensional number, which is determined based on the thermal properties of the coolant, is the Prandtl number, Pr. Unlike the previous nondimensional numbers, the Prandtl number is not affected by the flow or a length scale and is solely affected by the fluid properties and state. The Prandtl number is defined as

$$Pr = \frac{c_p \mu}{k} = \frac{\nu}{\alpha} \quad (4)$$

where c_p is the specific heat capacity, ν is the kinematic viscosity, and α is thermal diffusivity ($\alpha = k/\rho c_p$). Pr is largely used to compare different coolants to one another.

Further discussions on these nondimensional numbers and additional numbers can be found in [48], which focuses solely on jet impingement flow physics and heat transfer properties, and the metrics to quantify them. Jambunathan *et al.* [49], on the other hand, go in-depth on the heat transfer effects based on the Reynolds number.

B. Jet Physics

The dominant flow mechanism in jet impingement is the formation of vortex rings and eddies, which enhance mixing and, therefore, heat transfer. Almost directly after the jet nozzle, these vortex rings and eddies form in the jet stream. While there is no clear definition on the difference between eddies and vortices, generally, a vortex is a stable structure and eddies are quite unstable. Vortex rings do not necessarily constitute a turbulent flow, while eddies are identifiable structures within a turbulent flow. Vortex rings will stay the same size throughout a flow unless they encounter a solid body and are not generally vulnerable to disturbances. Eddies, on the other hand, range from larger eddies, which breakdown into smaller eddies [50], [51].

These flow mechanisms then affect the flow on the impingement plate, as they move from the impingement point, outwards. As the Reynolds number increases, the jet becomes more and more unstable [52]. While it has been found that vortex rings occur in low-Reynolds-number jets, they are generally noticed in transitional and turbulent flows. These eddies and vortex rings are needed for jet mixing and contribute to the relatively high heat transfer rates. It has been observed in the Nu experimental values reported that vortices cause a maximum Nu in two locations on the impinging area at higher Reynolds numbers, as observed in Fig. 3. Since these peaks are the regions of the highest heat removal, it is important to analyze their locations to increase heat transfer in critical areas.

More in-depth discussions can be found in reviews, which focus on the flow properties in jet impingement and the effect on heat transfer. Zuckerman and Lior [48] discuss these eddies and vortices, as well as the effects of turbulence on the heat transfer.

C. Types of Jets

1) Free-Surface Jets: Jets considered as free surface are unconfined flows. The fluid jet stream enters a gaseous region, normally air, after leaving the nozzle exit and displaces the preceding fluid as it impinges on the surface [53]. A free-surface jet is composed of three regions: free stream, stagnation point, and wall jet region (also commonly called the radial flow region) [54], which can be seen in Fig. 4(a).

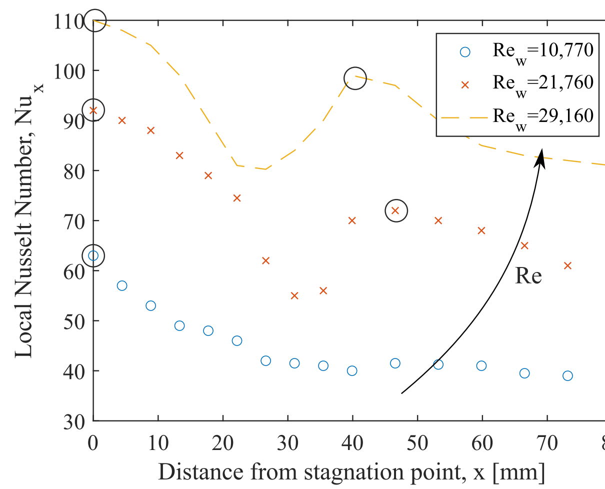

Fig. 3. Nusselt number for various Reynolds numbers [31], with the peaks circled.

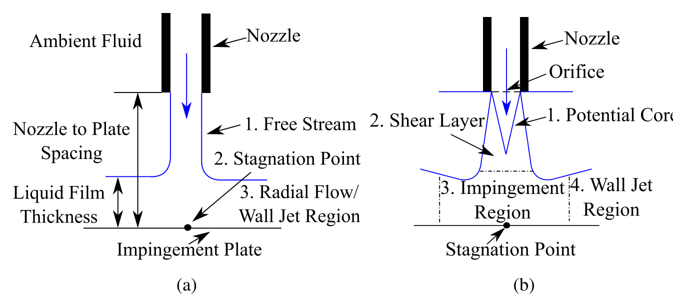

Fig. 4. Jet flow regions for a (a) free-surface liquid jet and (b) submerged liquid jet.

The free stream region of the jet occurs directly after the flow exits the orifice. Once the stream meets the impingement plate, the flow directly beneath the nozzle has a point of singularity, the stagnation point [55]. This is where the pressure is greatest, and there is negligible flow. The wall jet region occurs directly after the stagnation region, and the flow moves radially outward from the impingement area. Generally, the highest heat transfer occurs within the beginning of this region and may peak again or diminish as the flow moves outward. This wall jet region is also referred to as the liquid film, and the thickness is defined by the liquid–gas interface. The film thickness can be important in terms of heat transfer, since a larger thickness reduces the fluid velocity, and in turn, the heat transfer is also reduced [56].

Although there is extensive research on free-surface jet impingement [28], [29], [55], [57]–[61], few have been conducted for cooling applications of power electronics in electrified transportation. Gould *et al.* [39], however, studied submerged jets (explained in later sections) versus free-surface jets. They found that increasing the nozzle to plate spacing S, shown in Fig. 4(a),

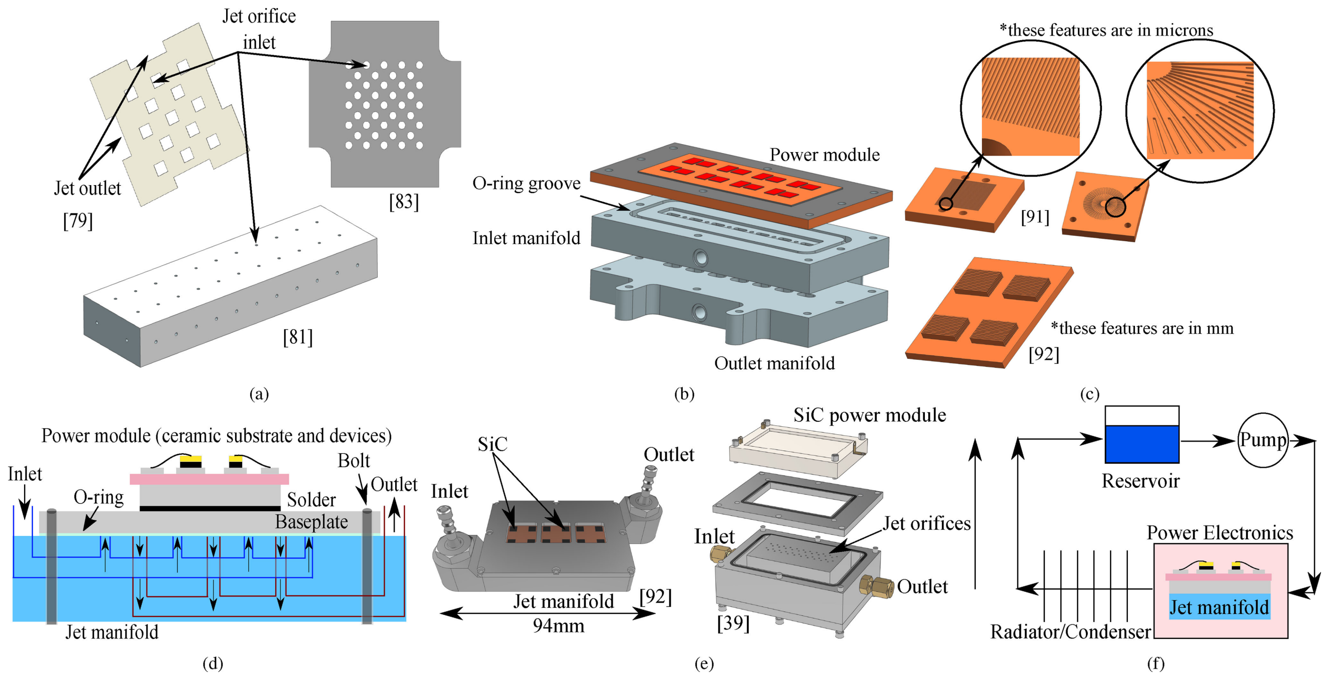

Fig. 5. Overview of jet impingement components and system: (a) jet orifices [79], [81], [83], (b) jet impingement manifold, (c) enhanced surfaces [91], [92], (d) jet impingement manifold mounted onto power module, (e) real-world examples of jet impingement power module cooling [39], [92], and (f) vehicle cooling loop.

results in the transition from submerged to free-surface jet. While the temperature of the impinging surface increased proportionately with the increase in S for the submerged jet, the change in S had very little effect on the temperature of impinging surface for the free-surface jet. The transition between submerged jet to free-surface jet occurred when the nozzle height became greater than the film thickness. Therefore, the jet interacted with the air region first, rather than disturbing the fluid region, before impinging on the surface.

Compared to submerged jets, free-surface jets generally have a larger nozzle to plate spacing, as well as reduced turbulence, which results in lower heat transfer [29]. Therefore, due to size constraints and the lower performance, free-surface jets are not normally used in automotive applications. Since there are few free-surface jet applications within the automotive industry, free-surface jets will not be further addressed, with an exception to synthetic and pulsating jets.

2) Submerged Jets: Submerged jets refer to flows, where the jet fluid is the same as the surrounding fluid [62]. For a turbulent, submerged jet, there are four main regions within the jet boundary and are shown in Fig. 4(b). The orifice, shown in Fig. 5(a), is the discharge area from the nozzle and is the beginning of the jet stream. Following the orifice is the shear layer and potential core. The shear layer is the area of jet fluid that starts to interact with the ambient fluid and turbulence is increased in this area [63]. The potential core is the region, where the centerline velocity is equal to the nozzle exit velocity and stays constant throughout this region [61]. In terms of heat transfer, the impingement plate should be in the potential core of the jet since the velocity greatly reduces after this area of the jet [28]. In terms of heat transfer rates, experimental data have also shown that submerged jets are more sensitive to S than free-surface jets, due to this potential core. While the potential core length depends on the Reynolds number, it is generally within 4–20 diameters long [61]. While the exact results may vary, it has been found that heat transfer is optimal when the nozzle to plate spacing is about equal to the diameter [28]–[31], [39], since the bulk of the impinging area, directly under the nozzle, is within the potential core. This can also be seen in [39] that as the nozzle-to-plate spacing increases above one jet diameter, the temperature of the impinging surface also increases.

Unless otherwise mentioned within this review, it can be assumed that all jet impingement designs utilize submerged jets. This is due to the improved heat transfer compared to free-surface jets, which is shown in [29], as well as [39]. This improved heat transfer is due to the increased turbulence caused by the jet stream interacting with stagnant fluid and is generated in the shear layer. As a note, in the literature, submerged and free-surface jets are not directly compared to one another, since different design parameters affect the two differently. It has been found, however, that the increased mixing in the potential core and shear layer increases the heat transfer performance of submerged jets, compared to free-surface jets, which do not mix with the surrounding air.

3) Synthetic and Pulsating Jets: Synthetic jets are unsteady jets caused by vibrations, piezoelectric device, or usage of a valve [64], [65]. In terms of heat transfer, there are many potential benefits to pulsating jets. Varying the jet flow allows surface renewal below the nozzle, which helps reduce bulk warming and can eliminate the stagnation point directly underneath the jet. Unlike steady jet impingement, pulsating jets result in heat transfer rates that change over time due to the pulsations.

Further discussions of these different jets, as well as their regions, can be found in jet impingement physics reviews. Zuckerman and Lior [48] discuss the physics of the three jets above, while the regions of jet impingement are further outlined in [56], [66], and [67]. Furthermore, synthetic jets, on their own, and their flow properties are reviewed in [68] and [69].

III. Jet Cooling Characteristics for Automotive Applications

Due to the enhanced heat transfer of jet impingement, several thermal management applications have been studied, with an increasing amount of research for power electronics in electrified transportation. For automotive applications, heat transfer, pressure drop, and reliability are important considerations for any cooling solution and are, therefore, analyzed for jet impingement designs.

A. Heat Transfer

Since both maximum temperature and temperature uniformity (temperature difference between semiconductor chips) of power modules can greatly affect the performance and efficiency [7], an adequate cooling strategy is required. Although the most commonly used power electronics cooling method is currently horizontal flow, vertical cooling methods, such as jet impingement, are being studied as potential options for improving heat transfer rates.

In order to determine the best cooling strategy, the heat transfer rates must be accurately analyzed. Generally, the three most common methods for determining heat transfer, for any cooling system, are analytical approaches, numerical modeling, and experimental testing. Analytical methods generally study the thermal network, which simplifies each component within the system, the most common of which is the lumped-parameter thermal network [70]–[72]. This approach uses the conductive thermal resistance of each material, the convective resistance of the cooling strategy, and the heat source to determine the temperature distribution of the system. Numerical modeling, on the other hand, is a software-based computing strategy that uses computation fluid dynamics (CFD) to study flow mechanisms, pressure, and heat transfer by using the continuity, momentum, and energy equations. Common CFD software are ANSYS-Fluent, ANSYS-CFX, COMSOL, and OpenFoam. Numerical methods are often used to verify the results computed using analytical methods, and Shukla and Dewan [66] go in-depth in reviewing the types and effects of using different computational methods.

Finally, experimental testing is generally used when the finalized designs have been chosen and are used to validate the results of the calculations. Experimental setups can have a large impact on the overall results, and therefore, care must be taken in ensuring that the setup is similar to the numerical models, as well as embodies a similar layout to the final application (e.g., power electronic cooling system in a hybrid vehicle).

Using analytical, numerical, and experimental methods, jet impingement has been proven to decrease the maximum temperature, compared to horizontal cooling methods [73], [74]. For jet impingement cooling, it has been found that as the Reynolds and Prandtl numbers are increased, vortex shedding and mixing of the fluid is increased, which allows for higher heat transfer [75], [76]. Along with increased Reynolds numbers, jet impingement offers the benefit of localized cooling. This allows for an increased temperature uniformity between dies, compared to horizontal methods [73], [77], which generally exhibit temperature rises in the coolant as it flows below the power module.

TABLE I
Power Density of Cooling Systems in [78]

	Air-Cooled Heat Sink	Liquid Cold-plate	Jet Impingement
Height (m)	0.059	0.015	0.05
Width (m)	0.122	0.127	0.062
Length (m)	0.174	0.177	0.122
Output Power (kW)	30	40	55
Power Density (W/cm^3)	24.0	118.6	145.4

As a comparison, Bhunia *et al.* [78] studied the thermal performance and pressure drop of an air-cooled heat sink, a liquid cold plate, and a jet impingement cooling cavity. The dimensions of each cooling system were provided, along with the output power the converter was able to achieve with each different heat sink. The power density of the system only including the volume of the heat sinks is reported in Table I. The baseplate of the power module measured 0.122 m $\times$ 0.062 m, and the air-cooled heat sink was made larger to take advantage of heat spreading. Due to the cooling limitations, the air-cooled heat sink only allowed 30-kW power output. The four-pass cold plate, however, saw an increase in power density by about a 79%. Finally, the jet impingement cooling cavity saw a maximum output power at 55 kW, which is an additional 21% increase in power density above the cold plate.

To further improve the heat transfer from jet impingement cooling, there are several parameters that can be optimized or modified. This includes the jet design configuration, the manufacturing method, the effective cooling area, and the material properties between the coolant and semiconductor chips. These topics will be discussed further, in the following sections, along with characterization methods for determining the heat flux and heat transfer. A summary of thermal performance for jet impingement cooling in the literature for power electronics applications is found in Table II. Here, the flow rate, jet hydraulic diameter, orifice shape, and any surface enhancements on the impingement surface are presented. Besides the nondimensional number Nu, the thermal performance of jet impingement is also recorded by the heat transfer coefficient and the thermal resistance in (5) and (6), respectively. Both of these are compared in Table II. Additionally, the orifice material and methodology for analyzing the jet cooling performance have been included

$$h = \frac{q''}{\Delta T} \tag{5}$$

where q'' is the heat flux of the devices and ΔT is the change in temperature from the device to the inlet coolant.

$$R_{\text{th}} = \frac{1}{hA} \tag{6}$$

TABLE II
JET IMPINGEMENT HEAT TRANSFER FOR POWER ELECTRONIC APPLICATIONS

Author/Year	Reynolds Number	Flow Rate (L/min)	Diameter (mm)	Orifice/ Material	Surface Enhancement	Methodology	Heat Transfer Coefficient (kW/m^2-K)	R_{th-jl} (K/W)
Narumanchi et al., 2012 [77]	8,000 - 43,000	2 - 10	1.4	Circular	Channels	ANSYS-Fluent	25 - 125	0.17 - 0.19
Papadopoulus et al., 2017 [79]	90 - 300	0.54	0.55 - 0.85	Square/ 3D Printed FC720	Micro-channels	Experimental/ COMSOL	7.05 - 130	0.25 - 0.55^{bl}
Parida et al., 2011 [80]	2,000	0.82 - 1	0.5 - 2	Circular/ Aluminum	Fins	Experimental/ ANSYS-CFX	0.03 - 29	0.28
Waye et al., 2014 [73]	500 - 2,500	10	1.4	Circular/ Machined Delrin	Microfins	Experimental	20	0.12 - 0.14
Wu et al., 2019 [81]	1,344 - 4,030	0.62 - 2	3	Circular/ Machined Aluminum	Channels	Experimental/ COMSOL	5 - 90	0.21 - 0.47
Agbim, 2017 [74]	8,462; 9,071	1.3 - 1.9	0.889; 1.56	Circular/ Lasered Acrylic	–	Experimental/ ANSYS	30.5; 35.7	0.04 - 0.88
Sabato et al., 2019 [82]	–	0.0326	–	Circular	–	Open-FOAM	40 - 75	–
Wei et al., 2019 [83]	10 - 3,500	0.05 - 1	0.01 - 1	Circular/ Micromachined PVC	–	Experimental/ CFD	62.5	0.25 - 2.5
Jörg et al., 2018 [84]	800 - 4,000	0.01 - 0.1	0.6	Circular	–	Experimental/ ANSYS Fluent	4 - 12	–
Skuriat et al., 2008 [85]	–	4	1	Circular	–	Experimental	7.5 - 22.5	–
Jörg et al., 2017 [86]	870	0.09 - 0.3	0.6 - 1.6	Circular/ PVC	–	Experimental/ ANSYS Fluent	1.72 - 5.83	–
Gould et al., 2014 [87]	–	0.156 - 0.195	0.2	Circular/ Stainless Steel	–	Experimental/ ANSYS Fluent	–	0.45

^{jl} Junction to liquid. ^{bl} Baseplate to liquid.

where A is cooling surface area. The thermal resistance is reported as the resistance between the junction to either the ambient, external case, or coolant.

1) Jet Design Effects: The manifold and nozzle design can greatly affect the heat transfer capabilities of the jet impingement cooling strategy, especially for power electronics. For both discrete power switches and power modules, heat loads are localized rather than bulk heating. These hotspots require effective cooling, and the cooling design must be customized for efficient operation of the power module.

The large-scale jet impingement design is the manifold, which consists of the inlet and outlet ports, as well as each of the jet nozzles, shown in Fig. 5(b). Both manifold and nozzle design parameters are adjusted to improve the heat transfer. The manifold parameters include the number of jets, the nozzle-to-plate spacing, the configuration of the jet placement, and the distance between jets. While the size of the power module is the main limiting factor for these considerations, crossflow effects [31] and location of hotspots [82] are also considered crucial for effective cooling. The jet locations must be placed to reduce the effect of jets interacting with one another, since single jets generally perform better than intermixing jets [31], [48].

Aside from the manifold design, the jet configuration can be optimized as well, including the jet diameter [82], number of inlets in one nozzle for sprays [88], and straight versus angled jets [80]. Also, the jet nozzle geometries can have some effect on the heat transfer, although the main impact results from the nozzle area. Therefore, if the nozzle area is the same, independent of the nozzle geometry, the heat transfer rates are comparable [37]. The trends found in literature for the effects of diameter and jet height are discussed in Section III.C below and shown in Fig. 6. For spray jets, it has been found that increasing the number of orifices in a nozzle will increase mixing, as well as heat transfer. This, however, decreases the cooling efficiency, defined by (7), since a greater fluid flow rate is required. The heat transfer and cooling efficiency resulting from the increased number of inlets is shown in Table III, which shows an increase in heat transfer coefficient by 2×, from two to four orifices.

TABLE III
HEAT TRANSFER COEFFICIENTS FOR TWO, THREE, AND FOUR SLOT JETS IN [88]

Number of Jets	Flow Rate (L/min)	Heat Transfer Coefficient (kW/m^2-K)	Cooling Efficiency
2	0.135	11	20%
3	0.1971	11.75	15%
4	0.2628	22.5	10%

This cooling efficiency from [88] has been defined as

$$\eta = \frac{\dot{q}''_w}{\mathrm{DC}\dot{m}''_f(c_p(T_b - T_f) + h_{fg})} \tag{7}$$

where $\dot{q}''_w$ is the heat flux on the cooling surface, DC is the injection duty cycle, $\dot{m}''_f$ is the mass flow rate, T_b is the boiling temperature of the coolant, T_f is the fluid temperature, and h_{fg} is the latent heat of vaporization. Since the application in [88] utilizes pulsating and two-phase spray jets, h_{fg} is used and will be further discussed in Section IV.

2) Manufacturing Effects: Although most jet impingement manifold designs are generally manufactured using subtractive manufacturing methods, there have been reports of an increase

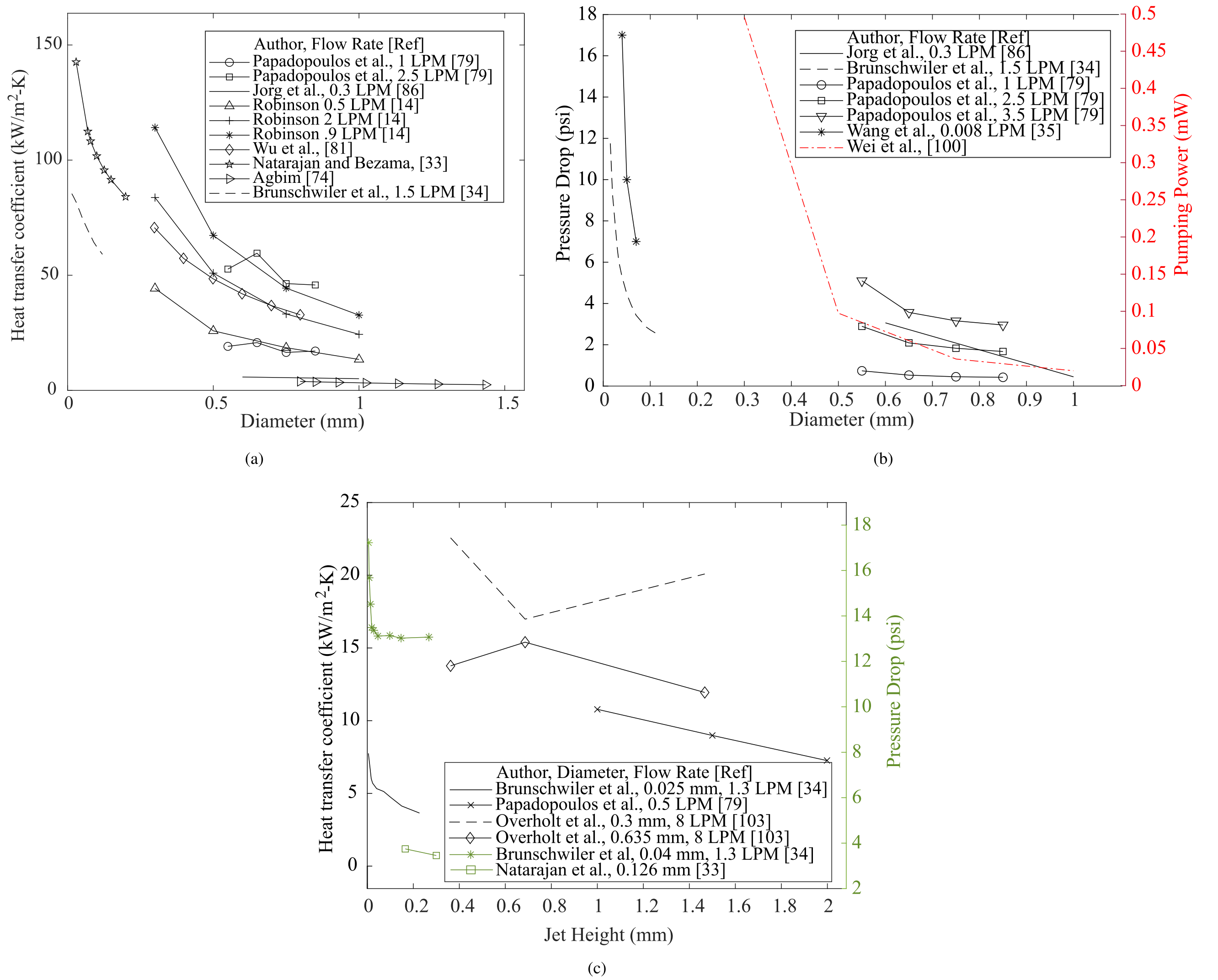

Fig. 6. Trends for power electronics jet impingement cooling. (a) Heat transfer coefficient versus jet diameter. (b) Pressure drop and pumping power versus jet diameter. (c) Heat transfer and pressure drop versus jet height.

in additive manufacturing as well. Additive manufacturing has started to gain more traction as an effective means of manufacturing small and complex designs. For several different applications, additive manufacturing is being studied to create jet impingement nozzles [89], [90]. Additive manufacturing, however, can result in nozzles with lower tolerances in jet diameter and imperfections left in the flow path of the manifold [79]. This is dependent on the capabilities of the additive technology, and with improved manufacturing, complex designs that enhance heat transfer can be achieved.

Additionally, unlike some traditional cooling methods, where the heat exchanger material has a large impact on the cooling performance, the jet impingement manifold thermal properties have little effect on the heat transfer. The manifold is not in the heat path between the coolant and the heat source. Major considerations for manifold manufacturing, however, include maximum temperature for the material (needs to withstand the high baseplate temperature), and additional insulation from ambient environment is needed if the air is warmer than the coolant.

3) Jet Impingement Cooling Surface Area Effects: Similarly, to other cooling strategies, jet impingement heat transfer can be improved with an increase in cooling surface area. Increasing the surface area can be achieved by introducing fins and channels [73], [77], [80], as well as cooling the sides of the power module baseplate [81]. Examples of these enhanced surface areas are shown in Fig. 5(c). Waye *et al.* [73] found that by introducing microfins to the impingement surface, the surface area was increased by about 11 times, which reduced the maximum and average temperatures of the semiconductor dies by 10 °C. For an inverter with 24 IGBTs dissipating 70 W each and 24 diodes at 35 W each, this resulted in a maximum device temperature of 107 °C, using a water ethylene glycol mix at 70 °C.

4) Thermal Interface Materials: Thermal interface materials (TIMs), shown in Fig. 2, are generally used between the substrate layers and the heat sink or baseplate, in power modules. TIMs are used to reduce the contact resistance between the two layers, by filling the air gaps [93]. These air gaps occur from surface roughness in the metal of the baseplate and substrate (usually copper or aluminum) during manufacturing. This grease layer, however, is the current bottleneck for thermal management of power electronics, and therefore, reducing this thermal resistance [84], [94] is being investigated. While studying a single MOSFET, cooled by jet impingement, without substrate or baseplate layers, Jörg *et al.* [84] found a 6000-W/m^2·K increase in the heat transfer coefficient by removing the grease layer. Although this cannot generally be implemented, unless the baseplate is removed, Narumanchi *et al.* [94] found that by reducing the thermal resistance of the TIMs by a factor of 5, the maximum temperature was decreased by 10 °C. This can be achieved by reducing the thickness of the TIM or by selecting interface materials with higher thermal conductivities.

5) Jet Impingement Heat Transfer Characterization: To study the heat transfer coefficient for the power electronic module, both numerically and experimentally, there are several methods of characterization. During characterization, the parameters that must be measured are the manifold inlet and outlet coolant temperature and the heat flux applied to the impinging surface.

Typically, to generate a heat source, a cartridge heater is embedded into the impinging surface [39], [95], which normally results in a bulk heat flux footprint, unlike real power modules. Metal heating rods have also been implanted into the impingement surface [81], which have a similar bulk heating distribution to the cartridge heaters. Generally, these two methods can provide comparisons between cooling methods and their heat transfer rates but cannot provide accurate temperature profiles that would be seen within a power module.

Some researchers have also used the actual power modules to generate the heat loads [73], [77]–[80], [87], [96]–[99]. This has the advantage of accurate junction temperatures of the semiconductor devices, as well as temperature distributions throughout the entire module. Testing with power modules, however, can result in module failures [98] and more expensive and high voltage testing.

Wei *et al.* [83], on the other hand, tested a multijet cooling array with thermal test chips to simulate power electronics. These thermal test chips use resistors to heat the chips and diodes to track the temperature. This allows for spacing between the heat sources and can be arranged on already established direct bonded copper (DBC) substrates and baseplates. With 75% of the chips used as heater cells and 100% used to map the temperature, Wei *et al.* found good agreement between the CFD model and experimental results.

B. Pressure Drop

Generally, it is found that improved heat transfer is counteracted with an increased pressure drop, since similar parameters affect both, like an increased flow rate [38]. Generally, while comparing channel flow to jet impingement cooling, the pressure drop increases [77], but this can be minimized by removing unnecessary flow paths within the jet impingement manifold [73]. Therefore, by optimizing parameters such as flow rate, nozzle design, and manifold design, the pressure drop can be reduced, while maintaining the high heat transfer capabilities of jet impingement. Pressure drop values using jet impingement for power electronics in electrified transportation, found in the literature, are shown in Table IV, along with the flow rate, jet diameter, and jet orifice.

The pumping power of the cooling system can be calculated using the pressure drop from the inlet to the outlet of the jet manifold, as follows:

$$W_P = \frac{\dot{m}}{\rho\eta}\Delta p \tag{8}$$

where $\dot{m}$ is the mass flow rate, ρ is the fluid density, η is the pump efficiency, and Δp is the pressure drop from the inlet to the outlet. The pumping power reported in the literature is included in Table IV.

In the study by Bhunia *et al.*, comparing the thermal performance between an air-cooled heat sink, cold plate, and jet impingement cooling, the pumping power was also recorded. The air-cooled heat sink required 46 W of blowing power during testing using a brushless dc backward curve fan. The four-pass liquid cold plate and the jet impingement cooling system both used a pump and required ranges of 24–32 W and 24–40 W, respectively. Therefore, the power required to pump a jet system can be comparable to conventional cooling systems [78].

By summing the pressure losses for each component in the cooling system, shown in Fig. 5(f), the total pressure drop can be calculated [102] and is highly dependent on the coolant flow rate. In most electric vehicles, the components and their cooling systems are integrated with one another to reduce weight and cost. These cooling systems generally include the electric motor, an on-board charger, the inverter, and other power electronic components, such as a battery, pumps, tubing, and valves. The reduced pressure drop in any component of the system, such as the jet impingement manifold, can lead to higher efficiency, as well as smaller pumps and lower pumping power. Therefore, the pressure losses should be reduced, while still effectively cooling each source of heat.

C. Heat Transfer and Pressure Drop Trends From Literature

While design parameters can have a large impact on the performance of any cooling design, especially jet impingement, trends can be seen from various jet designs under investigation. These trends found in the literature, specific to power electronics cooling, are presented in Fig. 6.

As can been seen from Fig. 6(a), smaller jet diameters increase the heat transfer, which also occurs for these power module applications [82]. This is due to the increased velocity within the nozzle and resulting velocity of the fluid impinging the heated surface. This increased heat transfer, however, is coupled with an increased pressure drop, shown in Fig. 6(b). Smaller diameters, however, can have high cooling performances at lower flow rates, which can greatly lower the required pumping power.

On the other hand, the jet-to-plate spacing, or height, S is shown to have more complicated trend, as shown in Fig 6(c). Generally, as S is reduced for submerged jets, both the heat transfer and pressure drop are increased. This trend, however, can be affected by the jet diameter. As shown by

TABLE IV
PRESSURE DROP RESULTS FROM LITERATURE FOR JET IMPINGEMENT OF SUBMERGED SINGLE-PHASE JETS

Author/Year	Reynolds Number	Flow Rate (L/min)	Diameter (mm)	Orifice	Pressure Drop (psi)	Pumping Power (W)
Bhunia and Chen, 2005 [96]	–	5.68 - 9.46	0.294	Slot	10 - 28	66 - 120
Narumanchi et al., 2012 [77]	8,000 - 43,000	2 - 10	1.4	Circular	0.156 - 2.81	–
Papadopoulus et al., 2017 [79]	90 - 300	0.54	0.55 - 0.85	Square	0.145 - 5.08	–
Gould et al., 2014 [87]	–	0.16 - 0.2	0.2	Circular	5	–
Sui et al., 2017 [99]	–	0.5 - 4	3.2; 6.2	Slot	0.409 - 5.421	–
Parida et al., 2011 [80]	2,000	0.82 - 1	0.5 - 2	Circular	0.003 - 2.9	0.005 - 0.11[a]
Gould et al., 2015 [39]	566 - 3,742	0.12 - 0.198	0.2	Circular	5	–
Waye et al., 2014 [73]	500 - 2,500	10	1.4	Circular	20	–
Mouawad et al., 2018 [97]	–	0.47 - 3	Not specified	Not specified	1.45 - 7.25	–
Agbim, 2017 [74]	8,462; 9,071	1.3 - 1.9	0.889; 1.56	Circular	15; 35	–
Jörg et al., 2018 [84]	800 - 4,000	0.01 - 0.1	0.6	Circular	0.145 - 6.52	0.001 - 0.075[a]
Wei et al., 2019 [100]	–	0.02 - 1	0.1 - 1	Circular	0.145 - 6.2	0.01-1[a]
Skuriat et al., 2008 [85]	–	4	1	Circular	–	0.15 - 10
Robinson et al., 2017 [101]	–	0.1 - 0.6	3.2	Ovular	1.45 - 36.26	0.05 - 2.375[a]
Wei et al., 2019 [83]	330 - 1,015	0.2 - 0.6	0.5; 2	Circular		0.4
Jörg et al., 2017 [86]	870	0.09 - 0.3	0.6 - 1.6	Circular	0.14 - 2.9	0.0002 - 0.1[a]

[a]Numerically calculated, η assumed to be 100%.

Overholt *et al.* [103], optimal heat transfer rates are when S is close the value of the diameter.

D. Reliability

Along with testing for improved heat transfer and minimizing pumping power, the reliability associated with the cooling method is also important. This is true for both the reliability of the cooling system itself and the increased or decreased reliability of the electronics based on the type of cooling system. Vehicles are expected to have at least a 15-year lifetime, perform under extreme temperature conditions (−40 to 140 °C underhood), and endure temperature cycling [104]. While the temperature of the power module determines the efficiency, elevated temperatures can also cause the devices to fail. Therefore, the thermal management solution should ensure that the power module never exceeds the maximum temperature of the device.

1) Power Module-Level Reliability: Neft *et al.* [98] studied the long-term effect of elevated junction temperatures to test the reliability of a converter system. These tests ran for 50 h on a bidirectional dc–dc converter with ambient temperatures as high as 120 °C and coolant temperature at 100 °C, while powered at 1 kW. It was found that after testing, for both directions of power flow, the jet impingement heat sink design, directly mounted to the baseplate, was more than adequate to prevent failure of the module. The tests, however, which used a commercial-off-the-shelf cold plate as the cooling solution, under the same conditions, caused failure within 2–3 h of testing [98]. Using the same tests as Neft *et al.* with a surrogate module, Gould *et al.* [39] determined that, while the SiC junction gate field-effect transistor and diodes could withstand the 175 °C operating temperatures, the surrounding components (e.g., solder joints and wire bond joints) could not. While lower target temperatures are not specific to jet impingement, when design limitations are set in place (e.g., high coolant temperatures), jet cooling has been found to meet these limitations that may not be met by conventional cooling. For example, although increasing the flow rate in the cold plate tested by Neft *et al.* [39] could increase heat transfer, the flow rate was limited by the overall cooling system, in which the inlet coolant entered from the coolant loop of the engine. Therefore, the higher heat transfer of the jet impingement cooling was able to keep the device below the maximum temperature of the module, throughout the entirety of the testing, even under these limitations.

Considering the maximum allowable temperature for each power electronic module, the heat dissipated can also be adjusted. If the cooling strategy can remove more heat, then the operating power of the device can be increased. Comparing jet impingement cooling to a cold plate and a microchannel cooling solution, Gould *et al.* [87] found that the heat dissipation allowed was increased by up to 178% for the jet cooling technique. At a fixed junction temperature of 175 °C and coolant temperature of 100 °C, the power dissipated by jet impingement was 167 W, compared to 60 and 99 W for the cold-pate and microchannels, respectively. This shows the increased reliability that results from jet impingement, compared to some more conventional cooling strategies for power electronics.

Furthermore, the impacts of solder fatigue were studied between a pin fin heat sink, jet impingement attached to the module baseplate, and jet impingement on the bottom substrate layer by O'Keefe and Vlahinos [105]. These tests were conducted by cycling junction temperatures from −40 to 140 °C. While they were testing the impact of the cooling system on solder fatigue, they found that the solder on the DBC was most likely to fail. When comparing the cooling systems, the cycles to failure was increased from 17 to 163 cycles for the pin fin cooling, to baseplate-cooled jet impingement, respectively. They also found that the cycles to failure for the IGBT solder and diode solder was increased by about 27% from the pin fin heatsink to the DBC jet impingement [105].

2) Cooling System-Level Reliability: Increased flow rates can cause erosion in the cooling system [106], especially with very small structures to enhance the surface area, like mini and microfins, as well as in the jet nozzles. Additionally, small jet diameters have the potential to clog, and depending on the fluid, this concern may be increased. To prevent clogging, however, Bhunia *et al.* [78] used a filter in their experimental setup.

In order to test degradation in the cooling system Waye *et al.* [73] and Narumanchi *et al.* [77], both preformed long-term reliability tests of the microfinned surfaces being impinged on. Both found no visual degradation of the fins, even up to 120 months of continuous impingement. Waye *et al.* used nickel-plated fins, which have a higher resistance to erosion than copper, and it was found that after the initial testing phases, the heat transfer performance stayed constant [73]. Also, Robinson *et al.* [101] used nickel cobalt for materials in contact with water since it has a higher resistance to degradation than copper. Furthermore, Ditri *et al.* [107] modeled the rate of erosion with ANSYS due to coolant impinging the baseplate. They found that for velocities up to 26 m/s, there was 20.2 μm/year being eroded, but was directly dependent on the containment particle diameter in the coolant.

E. Jet Impingement Integration

During installation of the jet impingement system, the jet manifold is mounted onto the power module and is normally either attached to the baseplate, as seen in Fig. 5(d) and (e), or onto the bottom substrate layer. Generally, the jet manifold is bolted to the module and an O-ring is placed to prevent leaking [39], [78], [98], [108], [109].

Although jet impingement heat sinks are more commonly mounted onto the baseplate of power modules, the performance is increased by integrating it into the power module. Skuriat and Johnson compared the thermal performance, in terms of heat transfer and thermal impedance, for jets attached to the baseplate and the bottom substrate layer. They found that removing the baseplate and TIM decreases the junction to coolant thermal resistance by 9% [85].

IV. Advanced Jet Impingement Technology for Power Modules

Although research has greatly improved the applicable capabilities for jet impingement, as a means of thermal management for power electronics, some applications require additional adjustments, further than those outlined above. Depending on the different cooling requirements, there are a wide variety of jet impingement cooling types. In the following subsections, advanced jet impingement technology investigated in electric vehicle power modules is outlined. This includes two-phase jet impingement, spray cooling, synthetic and pulsating jets, as well as integrated power modules that utilize jet impingement cooling.

A. Two-Phase Jet Impingement

Two-phase cooling maintains lower temperatures at higher heat fluxes than seen in single-phase cooling. Two-phase cooling utilizes both latent and sensible heat, while single-phase cooling only uses sensible heat, which is depicted in Fig. 7. As the heat flux increases, up to a critical heat flux (CHF), the temperature of the coolant does not increase while changing phases from liquid to gas during evaporation. Therefore, the coolant maintains the

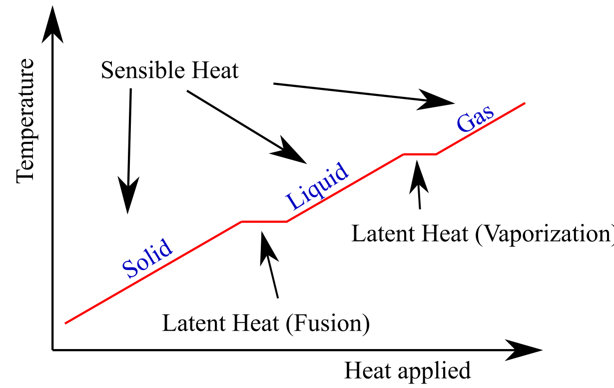

Fig. 7. Temperature curve as the heat applied is increased to two-phase cooling.

heat source or, in this case, the power module, at the same temperature when the fluid is evaporating. This allows higher heat transfer coefficients than single-phase jet impingement cooling. This may only occur up to a point, however, as the temperature will start to increase once the gaseous phase is reached. The CHF can be determined based on the coolant and flow properties and is reported often in the literature [40], [110]–[112].

Generally, two-phase cooling can dissipate from tens to thousands of W/cm^2 [113]. Dissipating large amounts of heat, however, results in large temperature gradients between the coolant and the heat source and, therefore, may not be ideal, depending on the temperature limits of the devices. For power modules, two-phase spray cooling is generally used from 150 to 400 W/cm^2 [88], [113], [114].

While numerically analyzing single-phase and boiling jet impingement on an IGBT package, Narumanchi *et al.* [38] found that boiling decreased the maximum temperature seen in the devices. Using an inlet water temperature of 105 °C and a pressure maintained at 135 kPa, two cases at 45 and 90 W/cm^2 were considered. It was found that introducing boiling into the jets decreased the maximum device temperature by 1.9 and 2.7 °C for the 45- and 90-W/cm^2 cases, respectively. Therefore, two-phase cooling has a higher potential for dissipating large heat fluxes.

Furthermore, the advancements in jet impingement boiling has been reviewed by Qui *et al.* [115]. The physics in jet boiling, trends between different design parameters, and the comparison between single and two-phase jet impingement are discussed. Overall, they found similar trends in terms of the heat transfer relationship to jet diameter and S, but higher heat transfer rates in two-phase jet cooling. It was also concluded that the heat transfer rates were increased significantly with the introduction of micro-pin-fins, as shown in [116]. In addition to increasing the surface area, surface enhancements also increase the bubble generation, which is very important in jet boiling [115].

B. Spray Cooling

Sprays are high-pressurized liquid streams forced through specialized nozzles that create droplets. While they do necessarily fall into the jet impingement umbrella, they have similar

TABLE V
SYNTHETIC JET IMPINGEMENT FOR ELECTRONICS COOLING

Author/Year	Reynolds Number	Hydraulic Diameter (mm)	Orifice	Frequency (Hz)	Pulsation Driver	Methodology/ Coolant	Nu
Pavlova et al., 2006 [120]	140 - 740	2	Circular	420; 1,200	Piezoelectric disk	Experimental/ Air	5 - 115%[a]
Jagannatha et al., 2009 [121]	162 - 2,781	1	–	250 - 1,000	–	ANSYS Fluent/ Air	4 - 24
Fang et al., 2010 [122]	95 - 475	0.1	Circular	10 - 150	Piezoelectric Actuator	Experimental/ Water	4.5 - 10.5
Abishek et al., 2020 [123]	568 - 2,809	–	Slot	0.25 - 0.5	Needle Valve	Experimental/ Water	28 - 54
Huang 2014 [124]	536 - 3,715	1	Square	153 - 4,880	Piezoelectric Stack	Experimental & ANSYS Fluent/ Air	20 - 100
Panão et al. 2012 [88]	–	0.4	Slot	3.75 - 60	Multijet Impingement Atomizer/ Spray Cooling	Experimental/ Methanol	5.6 - 7.4
Leena et al., 2015 [46]	10,000 - 20,000	1	Circular	0.1 - 0.5	Reciprocating Compressor	Experimental & ANSYS Fluent/ Air	19.5 - 32

[a]Percent improvement above natural convection.

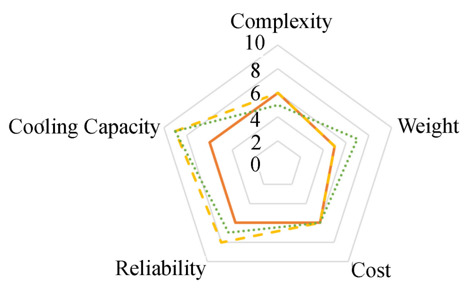

Fig. 8. Comparison of conventional cooling, spray cooling, and jet impingement for power electronics [118].

configurations and are sometimes considered an additional step from conventional jet impingement. The major difference between sprays and jet impingement is the nozzle type and the resulting fluid droplets. The sprays exit their nozzle in various droplet sizes, instead of the continuous stream in jet impingement. Sprays are also used to employ two-phase cooling [88], [113], [114] since the droplets make it easier to ensure evaporation.

Similar to jet impingement, spray cooling also possesses some drawbacks. Spray cooling pressure drops range from about 10 to 45 psi [111], which is slightly higher than jet impingement. This higher pressure is due to the specialized nozzles and high flow rates required to create sprays. However, this is counteracted with a higher heat removal. Also, similar to other liquid cooling methods, corrosion and erosion resistant materials must be selected to prevent the degradation of the thermal performance [117].

Generally, spray cooling can be more complex than conventional jet cooling, due to the high-pressurized nozzles, but can be lighter since less liquid is required. Ohadi and Qi [118] compared various future-trend cooling methods to one another, based on criteria, such as cost and cooling capacity. A spider chart from their data comparing complexity, weight, cost, reliability, and cooling capacity of conventional liquid cooling methods, spray cooling, and jet impingement is shown in Fig. 8. Each of the cooling systems generally costs the same to manufacture, while the reliability and cooling capacity of jet and spray cooling is higher than that of conventional cooling.

C. Synthetic and Pulsating Jets

As outlined in Section II, pulsating jets are generally utilized to improve heat transfer through the act of surface renewal. Different from conventional jet cooling, synthetic jets operate in various duty cycles of "ON" and "OFF." As the change in flow occurs, the stagnation point heat transfer is improved [119]. Pulsating jets can change their frequencies, injection times, and pulsation intensities to further enhance this phenomenon. These pulsations can be performed with both sprays and jet impingement. The heat transfer of synthetic jets in the literature is shown in Table V. Also shown is the method used to create the pulsations in the different synthetic jet applications. Similar to continuous jet impingement flow, the jet design parameters, as well as the time-averaged velocity, have an effect on the heat transfer in pulsating jets. The study by Pavlova and Amitay [120] showed a 5–115% increase in heat transfer compared to natural convection. Also, the improvement in the peak Nu was almost double that of a continuous jet. They found that the increased Reynolds number also increased the heat transfer, while the higher pulsation frequency had a higher peak Nu. At a distance of about 15 diameters from the stagnation point, the lower pulsation frequency had a higher Nu though. Pulsating jets, however, do not have much literature involving liquid coolants, especially so for electronics cooling. While it is a mature technology, liquid coolants in pulsating jets for power electronics are studied significantly less.

While studying two-phase sprays, Panão *et al.* [88] also studied the effect of the injection duty cycle, as well as injection times on the heat transfer and cooling efficiency. While the heat transfer was found to be the highest with a continuous spray (i.e., without pulsations), it had the lowest cooling efficiency. For the highest cooling efficiency and high heat transfer, it was found that the faster pulsations were favored, since there was less off time, while using less coolant than the continuous spray.

Generally, however, in the literature, there are mixed results on whether pulsating jets increase the heat transfer, and much of the current literature is on pulsating jets with air as the working coolant. While Azevedo *et al.* [125] found no significant improvements using pulsed jets, both O'Donovan and Murray as well as Hofmann *et al.* found improvements in some of their tests, but not all [126], [127].

Hofmann *et al.* [127], while studying jet impingement pulsations, concluded that jet performance was more sensitive to pulsation intensity rather than pulsation frequency and increased intensity resulted in higher heat transfer. The pulsation period was divided into 30 classes, in order to split the flow signal into the mean flow, the pulsating parts, and the turbulent parts. These classes are defined as the time passed since the beginning of each pulse cycle. The pulsation intensity, Pu_{eff}, is defined as follows:

$$Pu_{\text{eff}}(r, z) = \frac{A_{\text{eff}}(r, z)}{u(r, z)} \tag{9}$$

where r is the radial distance from the stagnation point, z is the axial distance from the nozzle, u is the axial component of the velocity, and A_{eff} is the effective amplitude and is defined as

$$A_{\text{eff}}(r, z) = \sqrt{\frac{1}{K-1}\sum_{k=1}^{K}|u_k - u|^2} \tag{10}$$

where K is the number of classes and k is the phase angle range. While they found that simply changing the frequency of the pulsations did not improve the heat transfer, an increase in the pulsation intensity had favorable results. The pulsation intensity averages the velocity throughout the entire pulsation cycle, instead of just the velocity exiting the nozzle. Therefore, this overall increase in mean velocity allows for higher heat transfer rates.

Sheriff and Zumbrunnen [128], on the other hand, used both sinusoidal and square pulse profiles. For a sinusoidal pulse profile, the time averaged Nu_0 was reduced by as much as 17% when the pulse magnitude was large. The pulse magnitude is defined as the pulse amplitude (the difference between the maximum and mean velocity) over the mean flow velocity. These Nu reductions decreased as the flow moved away from the stagnation region though. The jets utilizing the square-pulse profile (ON/OFF pulsations), however, resulted in 33% enhancement for the Nu at the stagnation region for a Strouhal number greater than 0.26, using (3), due to the boundary layer renewal. This enhancement was decreased with increasing frequency.

Therefore, although there are improved heat transfer rates with surface renewal in synthetic jets, the correct parameters must be customized for these effects to occur. While the complexity of the cooling system may increase, due to the added components (i.e., pulsation driver), higher cooling performance is possible.

D. *Integrated Cooling Through Jet Impingement*

As component integration in electric powertrains becomes increasingly favorable, a more efficient thermal management strategy must be implemented. For example, it is common to see the inverter integrated into the housing of the motor, which will inevitably result in higher heat dissipations.

De Lillo *et al.* [27] investigated the cooling system of the electric motor and inverter. In order to reduce the volume, the power modules were mounted on the endplate of the permanent magnet motor. The thermal management system consisted of jet impingement cooling for the power modules and the jet manifold outlet coolant flooding the stator windings. This compact design required large heat removal, which was successful using jet impingement with a 50–50 water glycol mix. Although the jet impingement design itself is considered conventional, in this case, the integration of the two systems is newer technology.

Similar to other advanced jet impingement technology, component integration can be more complex. The reduction in separate parts, however, reduces the volume and weight, both important parameters for making electrified transportation competitive. While the increased heat dissipations can also pose a concern, increased cooling performance, like jet impingement, has been found to allow for integrated components.

V. Gaps and Challenges

Although the work on liquid jet impingement cooling for automotive applications is gaining more attention, there are still gaps in the research that would enable faster implementation of the hotspot cooling strategy. A few of these gaps and challenges will be addressed in the following subsections.

A. *Jet Impingement Design Enhancements*

Since jet impingement for electric vehicle power modules has only been studied for the past 10–15 years, much of the research involved focuses on comparing a single jet impingement design to conventional cooling methods [14], [73], [77], [87]. Although these comparisons provide details on jet impingement performance compared to current cooling methods, more analysis is required to obtain the highest performance achievable.

Optimizing jet impingement design parameters to improve the heat transfer rates and reduce the pressure drop of the cooling system can allow for more efficient jet impingement cooling solutions. This process can be done by using optimization software, as well as comparing different jet impingement designs and selecting the highest performing solution. With such small and complex designs, the performance of the manifold is highly based on the different design parameters; therefore, these must be analyzed and compared to one another.

B. *Transient Heat Loads and Drive Cycles*

Although thermal modeling, under transient operation, such as a drive cycle, is available for vehicle testing of power modules [2], [129], [130], there is limited testing for comparing cooling designs, especially for jet impingement. In the literature of jet impingement, especially in vehicle testing, a constant heat flux is generally used, instead of fluctuating heat loads, or drive cycles. Although these constant heat loads are easier to model and experimentally test, they are ideal solutions and will likely have lower performance once implemented into a vehicle. This is due to thermal capacitance and increased switching losses not being accounted for during high power dissipation and overcooling of the system at lower power.

This issue can be addressed by numerically analyzing different heat loads and experimentally testing with computer simulated drive cycles, with the resulting power loads applied to the power modules or heat source. Therefore, resulting in a more comprehensive analysis of the performance of the power module, once placed in the vehicle. Testing at different heat loads will provide additional feedback for any potential performance issues (i.e., temperature build-up in extended testing).

C. Control-Based Work

While there are mentions to optimization of jet design parameters and control in the literature [74], [80], [131]–[133], there is not much research on how this could be implemented during transient heat loading, specifically for automotive applications. Control-based work, which utilizes a feedback loop, could be implemented during transient loads in testing and during vehicle operation. This control-based strategy could potentially improve heat transfer, during high heat loads, by modifying the flow rate or even pulsations accordingly. Also, lowering the supplied flow rate when the power module is at low temperatures could improve the cooling system's efficiency. By providing higher performance, as well improving efficiency, this could decrease overall costs in automotive applications [134].

VI. Conclusion

With increasingly high heat fluxes applied in power modules in the transportation sector, new cooling solutions with high heat transfer capabilities are required. Currently, the majority of electric vehicles utilize horizontal cooling techniques, but as the power densities are increased, these cooling methods will become inadequate. Liquid jet impingement is an attractive cooling technique due to the improved thermal performance and has been tested numerically and implemented experimentally. Although it is currently not implemented in industry, research shows very promising results as a thermal management technique.

The jet impingement design, manufacturing methods, the materials in the power module, and the effective cooling surface area all have an impact on the heat transfer coefficient while cooling power electronics. Jet impingement, however, has proven to keep the maximum temperature of the dies and temperature difference between dies below critical values. On top of conventional jet impingement designs for power electronics modules, advanced jet impingement techniques can be applied for higher heat transfer rates, including spray jets and synthetic jets.

Although there is a significant amount of research on jet impingement, further research is required for automotive applications, specifically. Current jet impingement designs are likely overdesigned for small dies in power modules, due to the lack of drive cycle testing and fluctuating heat loads. Further research investigating transient heat loading could improve the cooling efficiency. Overall, jet impingement is considered an attractive cooling option for power module cooling, within electric vehicles. Designs are being investigated to enhance heat transfer while reducing pressure drop, which is necessary as high heat fluxes are expected in future power electronic applications.

Jet impingement cooling has been shown to improve the performance of power electronics. While some applications have been found to increase the pressure drop from conventional cooling, jet impingement can improve the heat transfer performance and reliability. Additionally, it has been found to be versatile and customizable, depending on the application.

References

[1] A. Emadi, *Advanced Electric Drive Vehicles*. Boca Raton, FL, USA: CRC Press, Oct. 2014.

[2] A. Kempitiya and W. Chou, "An electro-thermal performance analysis of SiC MOSFET vs Si IGBT and diode automotive traction inverters under various drive cycles," in *Proc. 34th Annu. Semicond. Thermal Meas. Manage. Symp.*, San Jose, CA, USA, Mar. 2018, pp. 213–217.

[3] S. Mao, R. Ramabhadran, J. Popovic, and J. A. Ferreira, "Investigation of CCM boost PFC converter efficiency improvement with 600 V wide band-gap power semiconductor devices," in *Proc. IEEE Energy Convers. Congr. Expo.*, Montreal, QC, Canada, Sep. 2015, pp. 388–395.

[4] *Measuring HEXFET MOSFET Characteristics*, Int. Rectifier, El Segundo, CA, USA, 2004.

[5] Z. Chen, Y. Yao, M. Danilovic, and D. Boroyevich, "Performance evaluation of SiC power MOSFETs for high-temperature applications," in *Proc. 15th Int. Power Electron. Motion Control Conf.*, Novi Sad, Serbia, Feb. 2012, pp. DS1a.8-1–DS1a.8-9.

[6] M. Musallam, C. M. Johnson, C. Yin, H. Lu, and C. Bailey, "Real-time comparison of power module failure modes under in-service conditions," in *Proc. 13th Eur. Conf. Power Electron. Appl.*, Barcelona, Spain, Sep. 2009, pp. 1–10.

[7] *6th-Generation V-Series IGBT Module Application Manual*, Fiji Electric Co., Ltd., Tokyo, Japan, 2011.

[8] C. Qian *et al.*, "Thermal management on IGBT power electronic devices and modules," *IEEE Access*, vol. 6, pp. 12 868–12884, 2018.

[9] M. Pecht, *Handbook of Electronic Package Design*. New York, NY, USA: Marcel Dekker, 1991.

[10] J. Broughton, V. Smet, R. R. Tummala, and Y. K. Joshi, "Review of thermal packaging technologies for automotive power electronics for traction purposes," *J. Electron. Packag.*, vol. 140, pp. 1–11, Jul. 2018.

[11] Y. P. Zhang, X. L. Yu, Q. K. Feng, and R. T. Zhang, "Thermal performance study of integrated cold plate with power module," *Appl. Thermal Eng.*, vol. 29, nos. 17/18, pp. 3568–3573, Dec. 2009.

[12] I. Mudawar, "Assessment of high-heat-flux thermal," *IEEE Trans. Compon. Packag. Technol.*, vol. 24, no. 2, pp. 122–141, Jun. 2001.

[13] *Top-Side Cooled 650 V E-Mode GaN Transistor*, GaN Systems, Ottawa, ON, Canada, 2020.

[14] A. J. Robinson, "A thermal-hydraulic comparison of liquid, microchannel and impinging liquid jet array heat sinks for high-power electronics cooling," *IEEE Trans. Compon. Packag. Technol.*, vol. 32, no. 2, pp. 347–357, Jun. 2009.

[15] C. M. Johnson, A. Castellazzi, R. Skuriat, P. Evans, J. Li, and P. Agyakwa, "Integrated high power modules," in *Proc. 7th Int. Conf. Integr. Power Electron. Syst.*, Nuremberg, Germany, Mar. 2012, pp. 1–10.

[16] A. Blinov, D. Vinnikov, and T. Lehtla, "Cooling methods for high-power electronic systems," *Sci. J. Riga Tech. Univ. Power Elect. Eng.*, vol. 29, no. 1, pp. 79–86, Oct. 2011.

[17] A. Royne and C. J. Dey, "Effect of nozzle geometry on pressure drop and heat transfer in submerged jet arrays," *Int. J. Heat Mass Transfer*, vol. 49, nos. 3/4, pp. 800–804, Feb. 2006.

[18] H. M. Bahaidarah, "Experimental performance evaluation and modeling of jet impingement cooling for thermal management of photovoltaics," *Sol. Energy*, vol. 135, pp. 605–617, Oct. 2016.

[19] J. Barrau, J. Rosell, D. Chemisana, L. Tadrist, and M. Ibañez, "Effect of a hybrid jet impingement/micro-channel cooling device on the performance of densely packed PV cells under high concentration," *Sol. Energy*, vol. 85, pp. 2655–2665, Nov. 2011.

[20] R. Nadda, A. Kumar, and R. Maithani, "Efficiency improvement of solar photovoltaic/solar air collects by using impingement jets: A review," *Renewable Sustain. Energy Rev.*, vol. 93, pp. 331–353, Oct. 2018.

[21] R. Chauhan, T. Singh, N. S. Thakur, N. Kumar, R. Kumar, and A. Kumar, "Heat transfer augmentation in solar thermal collectors using impinging air jets: A comprehensive review," *Renewable Sustain. Energy Rev.*, vol. 82, no. 3, pp. 3179–3190, Feb. 2018.

[22] J. Jacobs, J. Tripp, D. Underwood, and C. Lengsfeld, "Optimization of micro-textured surfaces for turbine vane impingement cooling," in *Proc. ASME Turbo Expo.*, San Antonio, TX, USA, Jun. 2013, pp. 1–8.

[23] A. R. Ali and I. Janajreh, "Numerical simulation of turbine blade cooling via jet impingement," in *Proc. 7th Int. Conf. Appl. Energy*, Abu Dhabi, United Arab Emirates, Aug. 2015, vol. 75, pp. 3220–3229.

[24] F. Tong, W. Gou, Z. Zhao, W. Gao, H. Li, and L. Li, "Numerical investigation of impingement heat transfer on smooth and roughened surfaces in a high-pressure turbine inner casing," *Int. J. Thermal Sci.*, vol. 149, pp. 1–18, Mar. 2020.

[25] N. A. Mostafa, "Numerical investigation of a single jet impingement on a flat surface using a cubic k-ϵ non-linear eddy viscosity model, to predict the effect of cooling on gas turbine blades," in *Proc. 3rd Int. Conf. Energy Environ.: Adv. Towards Global Sustainability*, Malacca, Malaysia, Dec. 2009, pp. 226–231.

[26] A. Sarkar and N. Nittin and M. V. Karwe, and R. P. Singh, "Fluid flow and heat transfer in air jet impingement in food processing," *J. Food Sci.*, vol. 69, no. 4, pp. 113–122, May 2004.

[27] L. De Lillo, B. Ahmadi, L. Empringham, M. Johnson, J. Espina, and R. Abebe, "Next generation integrated drive, NGID: A novel approach to thermal and electrical integration of high power density drives in automotive applications," in *Proc. IEEE Energy Convers. Congr. Expo.*, Portland, OR, USA, Sep. 2018, pp. 1228–1232.

[28] D. J. Womac, F. P. Incropera, and S. Ramadhyani, "Correlating equations for impingement cooling of small heat sources with multiple circular liquid jets," *J. Heat Transfer*, vol. 116, no. 2, pp. 482–486, May 1994.

[29] D. J. Womac, S. Ramadhyani, and F. P. Incropera, "Correlating equations for impingement cooling of small heat sources with single circular liquid jets," *J. Heat Transfer*, vol. 115, no. 1, pp. 106–115, Feb. 1993.

[30] S. V. Garimella and R. Rice, "Confined and submerged liquid jet impingement heat transfer," *J. Heat Transfer*, vol. 117, no. 4, pp. 871–877, Nov. 1995.

[31] N. R. Saad, S. Polat, and W. J. Douglas, "Confined multiple impinging slot jets without crossflow effects," *Int. J. Heat Fluid Flow*, vol. 13, no. 1, pp. 2–14, Mar. 1992.

[32] S. V. Garimella and B. Nenaydykh, "Nozzle-geometry effects in liquid jet impingement heat transfer," *Int. J. Heat Mass Transfer*, vol. 39, no. 14, pp. 2915–2923, Sep. 1996.

[33] G. Natarajan and R. J. Bezama, "Microjet cooler with distributed returns," *Heat Transfer Eng.*, vol. 28, nos. 8/9, pp. 779–787, Jul. 2007.

[34] T. Brunschwiler *et al.*, "Direct liquid jet-impingement cooling with micronsized nozzle array and distributed return architecture," in *Proc. Thermal Thermomech. Proc. 10th Intersoc. Conf. Phenomena Electron. Syst*. San Diego, CA, USA, May 2006, pp. 196–203.

[35] E. N. Wang *et al.*, "Micromachined jets for liquid impingement cooling of VLSI chips," *J. Microelectromech. Syst.*, vol. 13, no. 5, pp. 833–842, Oct. 2004.

[36] D. W. Colucci, R. Viskanta, and W. Lafayette, "Effect of nozzle geometry on local convective heat transfer to a confined impinging air jet," *Exp. Thermal Fluid Sci.*, vol. 13, no. 1, pp. 71–80, Jul. 1996.

[37] D. Singh, B. Premachandran, and S. Kohli, "Effect of nozzle shape on jet impingement heat transfer from a circular cylinder," *Int. J. Thermal Sci.*, vol. 96, pp. 45–69, Oct. 2015.

[38] S. V. J. Narumanchi, V. Hassani, and D. Bharathan, "Modeling single-phase and boiling liquid jet impingement cooling in power electronics," Nat. Renewable Energy Lab., Golden, CO, USA, Tech. Rep. NREL/TP-540-38787, 2005.

[39] K. Gould, S. Cai, C. Neft, and A. Bhunia, "Liquid jet impingement cooling of a silicon carbide power conversion module for vehicle applications," *IEEE Trans. Power Electron.*, vol. 30, no. 6, pp. 2975–2984, Jun. 2015.

[40] C. Xia, "Spray/jet cooling for heat flux high to 1 kW/cm^2," in *Proc. 28th Annu. IEEE Semicond. Thermal Meas. Manage. Symp.*, San Jose, CA, USA, Mar. 2002, pp. 159–163.

[41] J. R. Rybicki and I. Mudawar, "Single-phase and two-phase cooling characteristics of upward-facing and downward-facing sprays," *Int. J. Heat Mass Transfer*, vol. 49, nos. 1/2, pp. 5–16, Jan. 2006.

[42] M. Visaria and I. Mudawar, "Application of two-phase spray cooling for thermal management of electronic devices," in Proc.*11th IEEE Intersoc. Conf. Thermal Thermomech. Phenomena Electron. Syst.,*Orlando, FL, USA, Jun. 2008, pp. 275–283.

[43] K. A. Estes and I. Mudawar, "Comparison of two-phase electronic cooling using free jets and sprays," *J. Electron. Packag.*, *Trans. ASME*, vol. 117, no. 4, pp. 323–332, Dec. 1995.

[44] P. K. Singh, S. K. Sahu, P. K. Upadhyay, and A. K. Jain, "Experimental investigation on thermal characteristics of hot surface by synthetic jet impingement," *Appl. Thermal Eng.*, vol. 165, pp. 1–12, Jan. 2020.

[45] J. Mohammadpour, M. M. Zolfagharian, A. S. Mujumdar, M. R. Zargarabadi, and M. Abdulahzadeh, "Heat transfer under composite arrangement of pulsed and steady turbulent submerged multiple jets impinging on a flat surface," *Int. J. Thermal Sci.*, vol. 86, pp. 139–147, Dec. 2014.

[46] R. Leena, R. V. Renjith, and M. J. Prakash, "Experimental and numerical investigations on steady and unsteady jet impingement cooling for high-power electronics," *IEEE Trans. Compon. Packag. Manuf. Technol.*, vol. 5, no. 5, pp. 636–640, May 2015.

[47] E. Laloya, Ó. Lucía, H. Sarnago, and J. M. Burdío, "Heat management in power converters: From state of the art to future ultrahigh efficiency systems," *IEEE Trans. Power Electron.*, vol. 31, no. 11, pp. 7896–7908, Nov. 2016.

[48] N. Zuckerman and N. Lior, "Jet impingement heat transfer: Physics, correlations, and numerical modeling," *Adv. Heat Transfer*, vol. 39, pp. 565–631, May 2006.

[49] K. Jambunathan, E. Lai, M. A. Moss, and B. L. Button, "A review of heat transfer data for single circular jet impingement," *Int. J. Heat Fluid Flow*, vol. 13, no. 2, pp. 106–115, Jun. 1992.

[50] J. Jeong and F. Hussain, "On the identification of a vortex," *J. Fluid Mech.*, vol. 285, pp. 69–94, Jan. 1995.

[51] P. K. Kundu and I. M. Cohen, *Fluid Mechanics*, 4th ed. Amsterdam, The Netherlands: Elsevier, 2008.

[52] S. C. Crow and F. H. Champagne, "Orderly structure in jet turbulence," *J. Fluid Mech.*, vol. 48, no. 3, pp. 547–591, Aug. 1971.

[53] M. Bieber, R. Kneer, and W. Rohlfs, "Self-similarity of heat transfer characteristics in laminar submerged and free-surface slot jet impingement," *Int. J. Heat Mass Transfer*, vol. 104, pp. 1341–1352, Jan. 2017.

[54] M. Molana and S. Banooni, "Investigation of heat transfer processes involved liquid impingement jets: A review," *Braz. J. Chem. Eng.*, vol. 30, no. 3, pp. 413–435, Jul./Sep. 2013.

[55] J. H. Lienhard, "Heat transfer by impingement of circular free-surface liquid jets," in *Proc. 18th Nat. 7th ISHMT-ASME Heat Mass Transfer Conf.*, Guwahati, India, Jan. 2006, pp. 1–16.

[56] M. A. Teamah and M. M. Khairat, "Heat transfer due to impinging double free circular jets," *Alexandria Eng. J.*, vol. 54, no. 3, pp. 281–293, Sep. 2015.

[57] K. Baghel, A. Sridharan, and J. S. Murallidharan, "Experimental and numerical study of inclined free surface liquid jet impingement," *Int. J. Thermal Sci.*, vol. 154, pp. 1–16, Aug. 2020.

[58] Y. Pan and B. W. Webb, "Heat transfer characteristics of arrays of free-surface liquid jets," *J. Heat Transfer*, vol. 117, no. 4, pp. 878–883, Nov. 1995.

[59] A. J. Robinson and E. Schnitzler, "An experimental investigation of free and submerged miniature liquid jet array impingement heat transfer," *Exp. Thermal Fluid Sci.*, vol. 32, no. 1, pp. 1–13, Oct. 2007.

[60] K. Baghel, A. Sridharan, and J. S. Murallidharan, "Numerical study of free surface jet impingement on orthogonal surface," *Int. J. Multiphase Flow*, vol. 113, pp. 89–106, Apr. 2019.

[61] T. L. Labus and E. P. Symons, "Experimental investigation of an axisymmetric free jet with an initially uniform velocity profile," NASA, Cleveland, OH, USA, Tech. Rep. NASA-TN-D-6783, May 1972.

[62] C. Agrawal, "Surface quenching by jet impingement—A review," *Steel Res. Int.*, vol. 90, no. 1, pp. 1–22, Aug. 2018.

[63] G. M. Carlomagno and A. Ianiro, "Thermo-fluid-dynamics of submerged jets impinging at short nozzle-to-plate distance: A review," *Exp. Thermal Fluid Sci.*, vol. 58, pp. 15–35, Oct. 2014.

[64] M. Amitay, "Synthetic jets and their applications for fluid/thermal systems," in *Proc. IUTAM Symp. Flow Controls MEMS*, London, U.K., Sep. 2006, pp. 77–93.

[65] R. Hou, C. Huang, and H. Zhu, "Experimental study on pulsation behavior of the ultrasonic vibration-assisted abrasive waterjet," *Int. J. Adv. Manuf. Technol.*, vol. 91, nos. 9–12, pp. 3851–3859, Jan. 2017.

[66] A. K. Shukla and A. Dewan, "Flow and thermal characteristics of jet impingement: Comprehensive review," *Int. J. Heat Technol.*, vol. 35, no. 1, pp. 153–166, Mar. 2017.

[67] J. H. V. Lienhard, "Liquid jet impingement," *Annu. Rev. Heat Transfer*, vol. 6, pp. 190–270, 1994.

[68] G. Krishan, K. C. Aw, and R. N. Sharman, "Synthetic jet impingement heat transfer enhancement—A review," *Appl. Thermal Eng.*, vol. 149, pp. 1305–1323, Feb. 2019.

[69] M. L. Hamman, "Pulsed flow jet impingement cooling: Evaluation of heat transfer performance," Master's thesis, Dept. Eng., Univ. Wisconsin-Milwaukee, Milwaukee, WI, USA, 2017.

[70] A. S. Bahman, K. Ma, P. Ghimire, F. Iannuzzo, and F. Blaabjerg, "A 3-D-lumped thermal network model for long-term load profiles analysis in high-power IGBT modules," *IEEE Trans. Emerg. Sel. Topics Power Electron.*, vol. 4, no. 3, pp. 1050–1063, Sep. 2016.

[71] M. Iachello *et al.*, "Lumped parameter modeling for thermal characterization of high-power modules," *IEEE Trans. Compon. Packag. Manuf. Technol.*, vol. 4, no. 10, pp. 1613–1623, Oct. 2014.

[72] D. Gerling and G. Dajaku, "Novel lumped-parameter thermal model for electrical systems," in *Proc. Eur. Conf. Power Electron. Appl.*, Dresden, Germany, Sep. 2005, pp. 1–10.

[73] S. K. Waye, S. Narumanchi, M. Mihalic, G. Moreno, K. Bennion, and J. Jeffers, "Advanced liquid cooling for a traction drive inverter using jet impingement and microfinned enhanced surfaces," in *Proc. Intersoc. Conf. Thermal Thermomech. Phenomena Electron. Syst.*, Orlando, FL, USA, May 2014, pp. 1064–1073.

[74] K. A. Agbim, "Single-phase liquid cooling for thermal management of power electronic devices," master's thesis, Dept. Mech. Eng., Georgia Inst. Technol., Atlanta, GA, USA, 2017.

[75] F. Alfieri, M. K. Tiwari, A. Renfer, T. Brunschwiler, B. Michel, and D. Poulikakos, "Computational modeling of vortex shedding in water cooling of 3D integrated electronics," *Int. J. Heat Fluid Flow*, vol. 44, pp. 745–755, Dec. 2013.

[76] D. Chatterjee and C. Sinha, "Effect of Prandtl number and rotation on vortex shedding behind a circular cylinder subjected to cross buoyancy at subcritical Reynolds number," *Int. Commun. Heat Mass Transfer*, vol. 70, pp. 1–8, Jan. 2016.

[77] S. Narumanchi, M. Mihalic, G. Moreno, and K. Bennion, "Design of light-weight, single-phase liquid-cooled heat exchanger for automotive power electronics," in *Proc. Intersoc. Conf. Thermal Thermomech. Phenomena Electron. Syst.*, San Diego, CA, USA, Jun. 2012, pp. 693–699.

[78] A. Bhunia, S. Chandrasekaran, and C. L. Chen, "Performance improvement of a power conversion module by liquid micro-jet impingement cooling," *IEEE Trans. Compon. Packag. Technol.*, vol. 30, no. 2, pp. 309–316, Jun. 2007.

[79] G. Papadopoulos and D. Torresin, "Evaluation of an integrated microcooling chip architecture for managing thermal concerns of a power electronics module," in *Proc. ASME Fluids Eng. Division Summer Meeting*, Waikoloa, HI, USA, Jul. 2019, pp. 1–10.

[80] P. R. Parida, S. V. Ekkad, and K. Ngo, "Impingement-based high performance cooling configurations for automotive power converters," *Int. J. Heat Mass Transfer*, vol. 55, no. 4, pp. 834–847, Jan. 2012.

[81] R. Wu, T. Hong, Q. Cheng, H. Zou, Y. Fan, and X. Luo, "Thermal modeling and comparative analysis of jet impingement liquid cooling for high power electronics," *Int. J. Heat Mass Transfer*, vol. 137, pp. 42–51, Jul. 2019.

[82] M. Sabato, A. Fregni, E. Stalio, F. Brusiani, M. Tranchero, and T. Baritaud, "Numerical study of submerged impinging jets for power electronics cooling," *Int. J. Heat Mass Transfer*, vol. 141, pp. 707–718, Oct. 2019.

[83] T. W. Wei *et al.*, "Experimental characterization and model validation of liquid jet impingement cooling using a high spatial resolution and programmable thermal test chip," *Appl. Thermal Eng.*, vol. 152, pp. 308–318, Apr. 2019.

[84] J. Järg, S. Taraborrelli, G. Sarriegui, R. De Doncker, and W. Rohlfs, "Direct single impinging jet cooling of a mosfet power electronic module," *IEEE Trans. Power Electron.*, vol. 33, no. 5, pp. 4224–4237, May 2018.

[85] R. Skuriat and C. M. Johnson, "Thermal performance of baseplate and direct substrate cooled power modules," in *Proc. 4th IET Conf. Pub.*, 2008, pp. 548–552.

[86] J. Jörg, S. Taraborrelli, E. Sabelberg, R. Kneer, R. De Doncker, and W. Rohlfs, "Hot spot removal in power electronics by means of direct liquid jet cooling," in *Proc. 16th Intersoc. Conf. Thermal Thermomech. Phenomena Electron. Syst.*, May/Jun. 2017, pp. 471–481.

[87] K. Gould, S. Q. Cai, C. Neft, and A. Bhunia, "Thermal management of silicon carbide power module for military hybrid vehicles," in *Annu. IEEE Semicond. Thermal Measur. Manage. Symp.*, San Jose, CA, USA, Mar. 2014, pp. 105–108.

[88] M. R. O. Panão, A. M. Correia, and A. L. N. Moreira, "High-power electronics thermal management with intermittent multijet sprays," *Appl. Thermal Eng.*, vol. 37, pp. 293–301, May 2012.

[89] T. W. Wei, H. Oprins, V. Cherman, I. De Wolf, E. Beyne, and M. Baelmans, "First demonstration of a low cost/customizable chip level 3D printed microjet hotspot-targeted cooler for high power applications," in *Proc. 69th Electron. Compon. Technol. Conf.*, Las Vegas, NV, USA, May 2019, pp. 126–134.

[90] B. Kwon, T. Foulkes, T. Yang, N. Miljkovic, and W. P. King, "Air jet impingement cooling of electronic devices using additively manufactured nozzles," *IEEE Trans. Compon. Packag. Manuf. Technol.*, vol. 10, no. 2, pp. 220–229, Feb. 2019.

[91] R. Jenkins, R. Lupoi, R. Kempers, and A. J. Robinson, "Heat transfer performance of boiling jet array impingement on micro-grooved surfaces," *Exp. Thermal Fluid Sci.*, vol. 80, pp. 293–304, Jan. 2017.

[92] U.S. Department of Energy, *Vehicle Technologies Office Annual Merit Review Results Report*. Washington, DC, USA: U.S. Dept. Energy, 2019.

[93] F. Sarvar, D. C. Whalley, and P. P. Conway, "Thermal interface materials—A review of the state of the art," in *Proc. 1st Electron. Syst.-Integr. Technol. Conf.*, Dresden, Germany, Sep. 2006, pp. 1292–1302.

[94] S. Narumanchi, M. Mihalic, K. Kelly, and G. Eesley, "Thermal interface materials for power electronics applications," in *Proc. 11th IEEE Intersoc. Conf. Thermal Thermomechanical Phenomena Electron. Syst*, Orlando, FL, USA, May 2008, pp. 395–404.

[95] M. R. O. Panão and A. L. N. Moreira, "Intelligent thermal management for full electric vehicles," in *Proc. Conf. Sustain. Develop. Energy, Water Environ. Syst.*, Dubrovnik, Croatia, Sep. 2011, pp. 45–56.

[96] A. Bhunia and C. L. Chen, "Jet impingement cooling of an inverter module in the harsh environment of a hybrid vehicle," in *Proc. ASME Summer Heat Transfer Conf.*, San Francisco, CA, USA, Jul. 2005, pp. 561–567.

[97] B. Mouawad, R. Skuriat, J. Li, C. M. Johnson, and C. DiMarino, "Development of a highly integrated 10 kV SiC MOSFET power module with a direct jet impingement cooling system," in *Proc. Int. Symp. Power Semicond. Devices ICs*, Chicago, IL, USA, May 2018, pp. 256–259.

[98] C. Neft, E. Hanna, V. Mehrotra, K. Gould, and A. Bhunia, "Design and testing of a 1 kW silicon-carbide (SiC) power module," in *Proc. 1st IEEE Workshop Wide Bandgap Power Devices Appl.*, Columbus, OH, USA, Oct. 2013, pp. 64–67.

[99] Y. Sui, H. Zhang, and P. Li, "Design analysis of minichannel heat sink with indented fins under impingement flow condition," in *Proc. Int. Conf. Electron. Packag. Technol.*, Harbin, China, Aug. 2017, pp. 336–341.

[100] T. Wei *et al.*, "High-efficiency polymer-based direct multi-jet impingement cooling solution for high-power devices," *IEEE Trans. Power Electron.*, vol. 34, no. 7, pp. 6601–6612, Jul. 2019.

[101] A. J. Robinson, W. Tan, R. Kempers, J. Colenbrander, N. Bushnell, and R. Chen, "A new hybrid heat sink with impinging micro-jet arrays and microchannels fabricated using high volume additive manufacturing," in *Proc. 33rd Annu. IEEE Semicond. Thermal Meas. Manage. Symp.*, San Jose, CA, USA, Mar. 2017, pp. 179–186.

[102] M. Cao, "Thermal and cooling systems modeling of powertrain for a plug-in parallel-through-the-road hybrid electric vehicle," master's thesis, Dept. Mech. Eng., Wayne State Univ., Detroit, MI, USA, 2014.

[103] M. R. Overholt, A. McCandless, K. W. Kelly, C. J. Becnel, and S. Motakef, "Micro-jet arrays for cooling of electronic equipment," in *Proc. 3rd Int. Conf. Microchannels Minichannels*, Toronto, ON, Canada, Jun. 2005, pp. 249–252.

[104] G. Moreno, S. Narumanchi, K. Bennion, S. K. Waye, and D. DeVoto, "Gaining traction: Thermal management and reliability of automotive electric traction-drive systems," *IEEE Electrific. Mag.*, vol. 2, no. 2, pp. 42–49, Jun. 2014.

[105] M. O'Keefe and A. Vlahinos, "Impacts of cooling technology on solder fatigue for power modules in electric traction drive vehicles," in *Proc. IEEE Veh. Power Propulsion Conf.*, Dearborn, MI, USA, Sep. 2009, pp. 1–10.

[106] U.S. Department of Energy, "Advanced power electronics and electric machinery program," U.S. Dept. Energy, Washington, DC, USA, Tech. Rep., 2007.

[107] J. Ditri, J. Hahn, R. Cadotte, M. McNulty, and D. Luppa, "Embedded cooling of high heat flux electronics utilizing distributed microfluidic impingement jets," in *Proc. ASME Int. Tech. Conf. Exhib. Packag. Integr. Electron. Photon. Microsyst.*, San Francisco, CA, USA, Jul. 2015, pp. 1–10.

[108] R. Wu, Y. Fan, T. Hong, H. Zou, R. Hu, and X. Luo, "An immersed jet array impingement cooling device with distributed returns for direct body liquid cooling of high power electronics," *Appl. Thermal Eng.*, vol. 162, pp. 1–11, Nov. 2019.

[109] M. K. Sung and I. Mudawar, "Experimental and numerical investigation of single-phase heat transfer using a hybrid jet-impingement/micro-channel cooling scheme," *Int. J. Heat Mass Transfer*, vol. 49, nos. 3/4, pp. 682–694, Feb. 2006.

[110] R. H. Chen, L. C. Chow, and J. E. Navedo, "Effects of spray characteristics on critical heat flux in subcooled water spray cooling," *Int. J. Heat Mass Transfer*, vol. 45, no. 19, pp. 4033–4043, Sep. 2002.

[111] L. Lin and R. Ponnappan, "Critical heat flux of multi-nozzle spray cooling in a closed loop," in *Proc. 37th Intersoc. Energy Convers. Eng. Conf.*, Washington DC, USA, Jul. 2002, pp. 341–346.

[112] J. Kim, "Spray cooling heat transfer: The state of the art," *Int. J. Heat Fluid Flow*, vol. 28, no. 4, pp. 753–767, Aug. 2007.

[113] I. Mudawar, D. Bharathan, K. Kelly, and S. Narumanchi, "Two-phase spray cooling of hybrid vehicle electronics," *IEEE Trans. Compon. Packag. Technol.*, vol. 32, no. 2, pp. 501–512, Jul. 2009.

[114] H. Bostanci, D. Van Ee, B. A. Saarloos, D. P. Rini, and L. C. Chow, "Thermal management of power inverter modules at high fluxes via two-phase spray cooling," *IEEE Trans. Compon. Packag. Manuf. Technol.*, vol. 2, no. 9, pp. 1480–1485, Sep. 2012.

[115] L. Qui, S. Dubey, F. H. Choo, and F. Duan, "Recent developments of jet impingement nucleate boiling," *Int. J. Heat Mass Transfer*, vol. 89, pp. 42–58, Oct. 2015.

[116] S. Ndao, Y. Peles, and M. K. Jensen, "Experimental investigation of flow boiling heat transfer of jet impingement on smooth and micro structured surfaces," *Int. J. Heat Mass Transfer*, vol. 55, pp. 5093–5101, 2012.

[117] D. D. Hall and I. Mudawar, "Experimental and numerical study of quenching complex-shaped metallic alloys with multiple, overlapping sprays," *Int. J. Heat Mass Transfer*, vol. 38, no. 7, pp. 1201–1216, May 1995.

[118] M. Ohadi and J. Qi, "Thermal management of harsh-environment electronics," in *Proc. 20th Annu. IEEE Semicond. Thermal Meas. Manage. Symp.*, San Jose, CA, USA, Mar. 2004, pp. 231–240.

[119] C. Camci and F. Herr, "Forced convection heat transfer enhancement using a self-oscillating impinging planar jet," *J. Heat Transfer*, vol. 124, no. 4, pp. 770–782, Aug. 2002.

[120] A. Pavlova and M. Amitay, "Electronic cooling using synthetic jet impingement," *J. Heat Transfer*, vol. 128, no. 9, pp. 897–907, Feb. 2006.

[121] D. Jagannatha, R. Narayanaswamy, and T. T. Chandratilleke, "Analysis of a synthetic jet-based electronic cooling module," *Numer. Heat Transfer, A, Appl.*, vol. 56, no. 3, pp. 211–229, Sep. 2009.

[122] R. Fang, W. Jiang, J. Khan, and R. Dougal, "Experimental heat transfer enhancement in single-phase liquid microchannel cooling with cross-flow synthetic jet," in *Proc. 14th Int. Heat Transfer Conf.*, Washington DC, USA, Aug. 2010, pp. 1–9.

[123] S. Abishek and R. Narayanaswamy, "Low frequency pulsating jet impingement boiling and single phase heat transfer," *Int. J. Heat Mass Transfer*, vol. 159, Oct. 2020, Art. no. 120052.

[124] L. Huang, "Synthetic jet flow and heat transfer for electronics cooling," Ph.D. dissertation, Dept. Mech. Eng., Univ. Minnesota, Minneapolis, MN, USA, May 2014.

[125] L. F. Azevedo, B. W. Webb, and M. Queiroz, "Pulsed air jet impingement heat transfer," *Exp. Thermal Fluid Sci.*, vol. 8, no. 3, pp. 206–213, Apr. 1994.

[126] T. S. O'Donovan and D. B. Murray, "Effect of acoustic excitation on the heat transfer to an impinging air jet," in *Proc. ASME/JSME Thermal Eng. Summer Heat Transfer Conf*, Vancouver, BC, Canada, Jan. 2007, pp. 183–191.

[127] H. M. Hofmann, D. L. Movileanu, M. Kind, and H. Martin, "Influence of a pulsation on heat transfer and flow structure in submerged impinging jets," *Int. J. Heat Mass Transfer*, vol. 50, nos. 17/18, pp. 3638–3648, Aug. 2007.

[128] H. S. Sheriff and D. A. Zumbrunnen, "Effect of flow pulsations on the cooling effectiveness of an impinging jet," *J. Heat Transfer*, vol. 116, no. 4, pp. 886–895, Nov. 1994.

[129] L. M. Tolbert, B. Ozpineci, S. K. Islam, and F. Z. Peng, "Impact of SiC power electronic devices for hybrid electric vehicles," in *Proc. Future Car Congr.*, Arlington, VA, USA, Jun. 2002, pp. 1–9.

[130] I. Aranzabal, I. M. De Alegria, N. Delmonte, P. Cova, and I. Kortabarria, "Comparison of the heat transfer capabilities of conventional single- and two-phase cooling systems for an electric vehicle IGBT power module," *IEEE Trans. Power Electron.*, vol. 34, no. 5, pp. 4185–4194, May 2019.

[131] S. Ndao, Y. Peles, and M. K. Jensen, "Multi-objective thermal design optimization and comparative analysis of electronics cooling technologies," *Int. J. Heat Mass Transfer*, vol. 52, nos. 19/20, pp. 4317–4326, Sep. 2009.

[132] M. Fabbri and V. K. Dhir, "Optimized heat transfer for high power electronic cooling using arrays of microjets," *J. Heat Transfer*, vol. 127, no. 7, pp. 760–769, Jul. 2005.

[133] A. G. Fedorov and J. M. Meacham, "Evaporation-enhanced, dynamically adaptive air (gas)-cooled heat sink for thermal management of high heat dissipation devices," *IEEE Trans. Compon. Packag. Technol.*, vol. 32, no. 4, pp. 746–753, Dec. 2009.

[134] T. Brunschwiler, H. Rothuizen, S. Paredes, B. Michel, E. Colgan, and P. Bezama, "Hotspot-adapted cold plates to maximize system efficiency," in *Proc. 15th Int. Workshop Thermal Investigations ICs Syst.*, Leuven, Belgium, Nov. 2009, pp. 150–156.

Samantha Jones-Jackson (Student Member, IEEE) received the B.S. degree in mechanical engineering from Michigan State University, East Lansing, MI, USA, in 2018. She is currently working toward the Ph.D. degree in mechanical engineering with McMaster University, Hamilton, ON, Canada.

Her industrial experience focused on automotive applications, during her undergraduate degree, where she worked with Delphi and McLaren as a Mechanical Engineer. Her research interests include thermal management techniques in power electronic modules and electric machines.

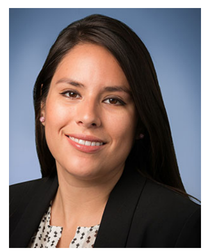

Romina Rodriguez (Member, IEEE) received the B.S. and M.S. degrees from the University of California, Berkeley, Berkeley, CA, USA, in 2010 and 2012 respectively, and the Ph.D. degree from McMaster University, Hamilton, ON, Canada, in 2019, all in mechanical engineering.

She was a Mechanical Engineer with the Thermal Design & Analysis Group, Hardware Engineering Department, Northrop Grumman, Palmdale, CA, USA, from 2012 to 2014. She is currently a Postdoctoral Fellow with the McMaster Automotive Resource Centre, McMaster University. Her research interests include thermal management of power electronics and electric machines and investigating energy harvesting technologies.

Ali Emadi (Fellow, IEEE) received the B.S. and M.S. degrees in electrical engineering (with highest distinction) from the Sharif University of Technology, Tehran, Iran, in 1995 and 1997, respectively, and the Ph.D. degree in electrical engineering from Texas A&M University, College Station, TX, USA, in 2000.

He is the Canada Excellence Research Chair Laureate with McMaster University, Hamilton, ON, Canada. He is also the holder of the NSERC/FCA Industrial Research Chair in Electrified Powertrains and Tier I Canada Research Chair in Transportation Electrification and Smart Mobility. Before joining McMaster University, he was the Harris Perlstein Endowed Chair Professor of Engineering and the Director of the Electric Power and Power Electronics Center and Grainger Laboratories, Illinois Institute of Technology, Chicago, IL, USA, where he established research and teaching facilities as well as courses in power electronics, motor drives, and vehicular power systems. He was the Founder, Chairman, and President of Hybrid Electric Vehicle Technologies, Inc.—a university spin-off company of the Illinois Institute of Technology. He is the President and Chief Executive Officer of Enedym, Inc., and Menlolab, Inc., -two McMaster University spin-off companies. He is the principal author/coauthor of more than 500 journal and conference papers as well as several books, including *Vehicular Electric Power Systems: Land, Sea, Air, and Space Vehicles* (Boca Raton, FL, USA: CRC Press, 2003), *Energy Efficient Electric Motors* (Boca Raton, FL, USA: CRC Press, 2004), *Uninterruptible Power Supplies and Active Filters* (Boca Raton, FL, USA: CRC Press, 2005), *Modern Electric, Hybrid Electric, and Fuel Cell Vehicles: Fundamentals, Theory, and Design* (2nd ed. Boca Raton, FL, USA: CRC Press, 2009), and *Integrated Power Electronic Converters and Digital Control* (Boca Raton, FL, USA: CRC Press, 2009). He is also the Editor of the books entitled *Handbook of Automotive Power Electronics and Motor Drives* (Boca Raton, FL, USA: CRC Press, 2005) and *Advanced Electric Drive Vehicles* (Boca Raton, FL, USA: CRC Press, 2014). He is the co-editor of the *Switched Reluctance Motor Drives: Fundamentals to Applications* (Boca Raton, FL, USA: CRC Press, 2018).

Dr. Emadi was the Inaugural General Chair of the 2012 IEEE Transportation Electrification Conference and Expo and has chaired several IEEE and SAE conferences in the areas of vehicle power and propulsion. He was the founding Editor-in-Chief of the IEEE TRANSACTIONS ON TRANSPORTATION ELECTRIFICATION from 2014 to 2020.